Transport measurements in granular niobium nitride cermet films

R. W. Simon,* B. J. Dalrymple,* D. Van Vechten, W. W. Fuller, and S. A. Wolf
Naval Research Laboratory, Washington, D.C. 20375
(Received 4 March 1987)

We have studied normal-state and superconducting transport properties in a granular cermet consisting of $B1$-structure NbN grains in a boron nitride insulating matrix. By varying the volume fraction of the two components we produced films (20–70 nm in thickness) that exhibited transport behavior in either of two distinct and mutually exclusive classes: "insulating" films with $\rho \sim \exp(-a/T^{1/2})$ which never went superconducting, and "superconducting" films with $\rho \sim \ln(T)$ from room temperature down to the superconducting transition. This latter logarithmic temperature dependence for the resistivity is also observed at low temperature when superconductivity is suppressed in high magnetic fields. Broad superconducting transitions are observed with a strong compositional dependence of the mean field critical temperature, T_{c0}. The Kosterlitz-Thouless two-dimensional (2D) topological phase transition at T_{2D} is observed in the superconducting samples both by the power-law behavior in current-voltage characteristics and by pure flux flow transport in high magnetic fields.

I. INTRODUCTION

In recent years considerable experimental and theoretical efforts have been expended in the study of inhomogeneous superconducting films. The systems studied have included amorphous films, granular films, and multilayer structures. Amorphous and granular films, in particular, have been extensively investigated for the effects of disorder and reduced dimensionality on both superconducting and normal-state properties. These systems often exhibit a metal-insulator transition that is conducive to the study of localization and electron-electron interaction effects.[1,2] Thin-film superconductors have also been a fertile ground for investigations of the two-dimensional (2D) topological phase transition (Kosterlitz-Thouless transition).[3–5]

In general, these systems have consisted of superconducting grains or regions embedded in an insulating matrix composed of oxides of the metallic component. Aluminum grains in aluminum oxide is a particularly well studied system.[2,4] Thin amorphous films of In/InO_x have also been investigated in detail.[6] Niobium nitride embedded in Nb_2O_5 has been extensively studied at the Naval Research Laboratory[3] and represents a particularly interesting system because of the high superconducting transition temperatures of the films and high critical magnetic fields. Such films were produced by chemically anodizing sputtered niobium nitride until only a very thin (~ 3 nm) layer of NbN grains embedded in an oxide matrix remained.[7]

The present work deals with a unique system consisting of a niobium nitride–boron nitride cermet. Cermets are micrgranular mixtures of insulating and metallic particles. Such systems allow for the continuous variation of the volume fraction f_i of each constituent. At each extreme ($f_i \sim 1$), the properties of the cermet are essentially that of a pure phase, but in between the system can either take on some sort of intermediate behavior or can exhibit behavior totally unique to the mixture. Cermets have practical applications[8,9] as well as being model systems for studies of such effects as the critical phenomena associated with percolation.[10] The NbN/BN cermet allows for the study of a high-critical-temperature superconducting granular system in which the insulating matrix is truly insulating and for which there is fine control over the properties of the films.

In this paper we report on the fabrication of the cermets and on detailed measurements of the temperature dependence of the resistivity of the cermet films. We have observed two distinct types of behavior depending on the relative concentration of the two film constituents. Nonsuperconducting films display a previously observed temperature dependence while the superconducting films exhibit a unique wide-range logarithmic temperature dependence of the resistivity. The superconducting films can be analyzed in terms of two-dimensional fluctuation theory at higher temperatures and in terms of Kosterlitz-Thouless (KT) theory at low temperatures. The KT transition temperature can be accurately determined by two independent means with good agreement.

II. SAMPLE PREPARATION

The cermets were prepared in an oil-free ultrahigh-vacuum system (base pressure $\sim 2\times 10^{-9}$ Torr) by reactive rf sputtering. The target consisted of a half disk of niobium and a half disk of boron nitride mounted side by side on a cooled copper block. The chamber was backfilled to a pressure of 68 Torr with argon and then nitrogen was bled in so that the total pressure was a constant 90 Torr during the deposition. The argon-to-nitrogen ratio was thus approximately 3:1. The 0.43-mm-thick sapphire substrates were heated to 1000 C by carbon strip heaters beneath the substrate table. Deposition rates on the order of 1.5 nm/min were obtained. Under such conditions, high-quality niobium nitride films can be formed on the substrates in the absence of the boron nitride target (we could cover the BN half of the target and sputter

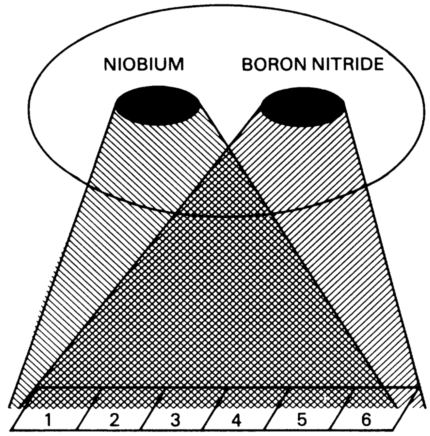

FIG. 1. Reactive rf sputtering from a split niobium and boron nitride target produced a spread in concentration of the components of the cermet on the substrates. Substrate 1 was mainly NbN, while substrate 6 was mostly BN.

from the Nb half through a hole in the shutter. Such depositions resulted in NbN films with a critical temperature of 16.5 K). For the split-target case, however, the metal-insulator composite material (cermet) was formed. Typical film thicknesses were 20-70 nm for these samples.

The two targets were symmetrically located near the center line of the substrate table which allowed the substrates to be arranged in a line extending from a point directly below the niobium target to a point directly below the boron nitride target (Fig. 1). Therefore, the composition of the resultant films varied from mostly niobium nitride to mostly boron nitride depending upon the position of the substrate. In this way a considerable spread in material properties could be studied from the result of a single deposition.

The films were then patterned using conventional photolithographic techniques (Shipley AZ1350J photoresist masking and CF_4 plasma or wet etching) into a form convenient for four-probe resistance measurements. We chose narrow (0.5-mm) strips of the material perpendicular to the direction of the compositional phase gradient. Over this width we expect very little variation of the sheet resistance based on the total change over each half-inch substrate.

III. CHARACTERIZATION OF FILMS

The sputtered cermets consist of fairly regular grains of NbN embedded in an amorphous insulating matrix presumably composed of boron nitride. X-ray-diffraction studies show the NbN to be $B1$-structure material with a typical lattice spacing of 4.38 Å, which is consistent with other films made in the same system. The x-ray studies did not reveal any reflections attributable to the BN in the films.

Transmission electron microscopy (TEM) was used to study the microstructure of the films with particular attention paid to the grain-size distribution. Figure 2 shows four micrographs of films from four different substrate locations from the same deposition. The first point to be made is that the films clearly consist of isolated, regular grains with only relatively small variations in size for a

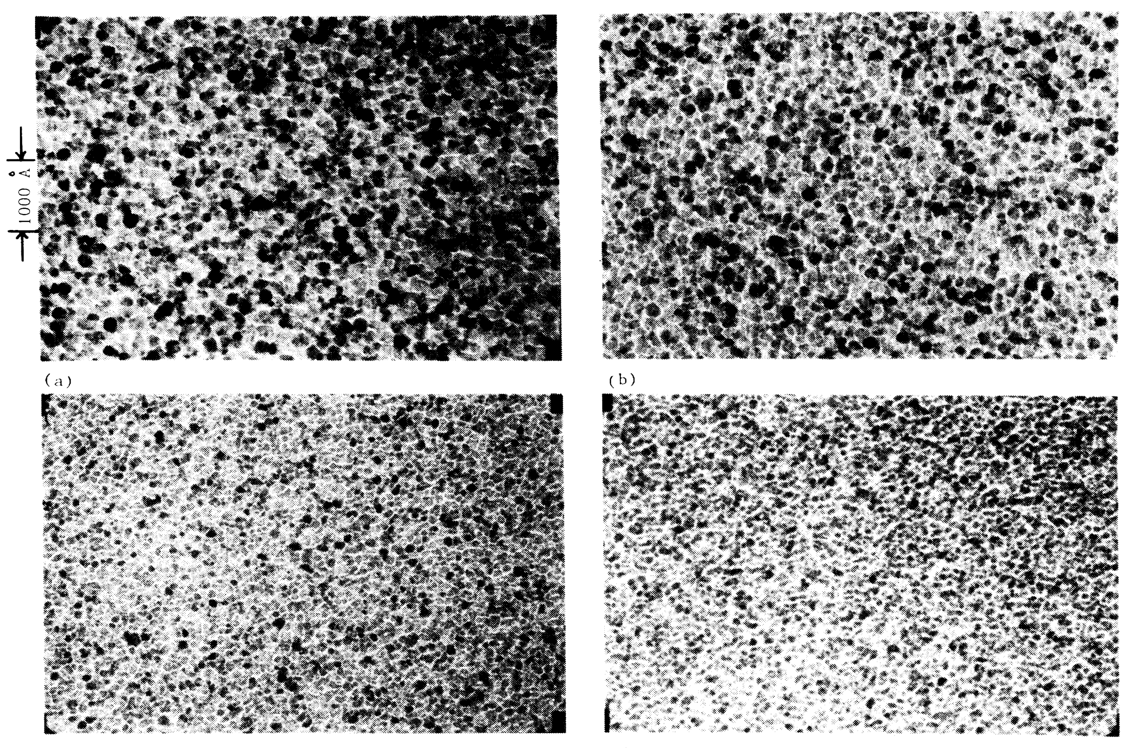

FIG 2. Micrographs of films at four different substrate locations. The substrate positions as referred to Fig. 1 are (a) 2, (b) 3, (c) 4, and (d) 5.

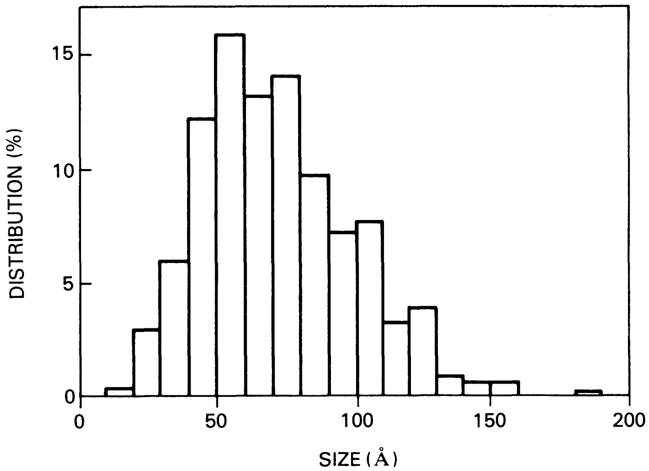

FIG. 3. A typical distribution for the grain size of a NbN/BN sample. The distribution was for a particular substrate position (substrate 2).

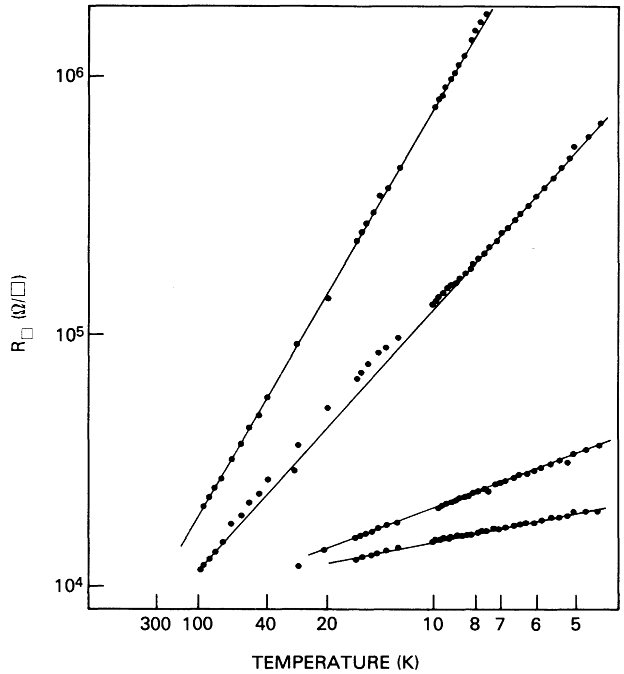

FIG. 4. The logarithm of the sheet resistance as a function of $1/\sqrt{T}$ for a variety of the nonsuperconducting samples. The lines are guides to the eye.

given film. The second point is that there is a pronounced variation in grain size from film to film; as the films progress from the niobium nitride–rich end to the boron nitride–rich end, the grains get significantly smaller. On the other hand, the intergrain spacing does not seem to vary nearly as much. What appears to be happening is that the grains nucleate in a similar fashion from film to film, but the effectively lower rate of NbN deposition on the BN-rich side results in smaller grains with the intervening spaces filled in with the insulating material.

The distribution of grain sizes can be analyzed from the TEM photos and such analysis demonstrates mean grain sizes from less than 4 to over 10 nm for the films studied. A typical distribution is shown in Fig. 3.

The electrical properties of the cermets vary strongly with the composition gradient. Different conduction mechanisms in cermet films are well known to occur depending on metal grain size[11] and such effects are present here. Measured resistivities of the films vary from about 100 $\mu\Omega$ cm on the NbN-rich side to immeasurably high values on the opposite end of the phase spread. Measurable samples could be made over a distance of 6–8 cm on the substrate table which was 10 cm from the target, and such samples had room-temperature sheet resistances from 100 to 20 000 $\Omega/\square$.

IV. NORMAL-STATE RESISTANCE

The cermets fall naturally into two groups: those that exhibit superconducting transitions and those that do not. This distinction carries with it other important characteristics of the films. In particular, the temperature dependence of the resistance of the films is well described by one of two relations, depending on the group to which the film belongs. The nonsuperconducting films are characterized by an exponential temperature dependence of the resistance, while the superconducting films exhibit a remarkable logarithmic temperature dependence. The superconducting films have room-temperature sheet resistances below 3000 $\Omega/\square$; the nonsuperconducting films have higher sheet resistances.

Figure 4 shows the sheet resistance of four of the nonsuperconducting films as a function of temperature plotted as the logarithm of $R_\square$ versus the inverse square root of the temperature. The films clearly obey a relationship of the form

$$R = R_0 e^{-(a/T^{1/2})} , \quad (1)$$

which is a temperature dependence that has been seen before in granular materials. Such a dependence has been attributed to either a thermally activated tunneling process[9,12] in which tunneling takes place between grains having charge whose distribution is thermally populated, or by a hopping conduction mechanism with Coulomb-energy effects.[13,14] The first explanation involves assumptions about the relationship between the grain-size distribution and intergrain spacings that are inappropriate for these films.[11] The second account of this type of resistivity behavior involves the incorporation of a "Coulomb gap"[14] in the density of states near the Fermi level into the Mott theory for variable-range hopping. In these samples, the above temperature dependence is clearly observable over three decades of resistance in the films and thus can be easily distinguished from other exponential laws such as $T^{-1/4}$ or $T^{-1/3}$ that are expected when conduction results from simpler hopping mechanisms.

The presence of this temperature dependence of the resistance of the cermet films turns out to be a clear empirical indicator that no superconducting transition will occur at lower temperatures. Films whose room-temperature resistances were near the cutoff value for superconductivity were measured down to below 100 mK in our dilution refrigerator and the exponential behavior persisted at all temperatures. Whatever the details of the conduction mechanism may be, an entirely different interaction appears to take hold for films of lower sheet resistance.

Aside from the fact that the lower-resistance films exhibit superconducting transitions (to be discussed in the next section), these cermets are still very nonmetallic in the sense that their resistance increases strongly with lowered temperature. However, the films no longer obey an exponential law, but rather are governed by a logarithmic relation of the form

$$R = R_0 \ln(T_0/T) . \tag{2}$$

Figure 5 shows the sample resistance (normalized to the room-temperature value) plotted against temperature on a logarithmic scale for two superconducting samples of very different sheet resistance. Notice the very good fit to the $\ln T$ dependence and, more importantly, the very large changes in resistance, especially for the high-resistance sample. In this case the resistance varies by 500% over a decade change in temperature, which is an enormous effect. The logarithmic dependence can be seen from as high as room temperature all the way down to the onset of superconducting fluctuations (typically around 20 K for these films). Moreover, when the superconductivity is suppressed by the application of a high magnetic field, this logarithmic dependence is observed down to the lowest temperatures measured (see Fig. 11).

Plots like Fig. 5 can be made for all the superconducting samples from which the slope—R_0 in the above equation—can be extracted. This characteristic resistance R_0 for each film is seen to vary systematically with other measured properties of the films including the critical temperature, room-temperature resistance, and, most interestingly, the peak resistance before the superconducting transition. For samples prepared in the same run, the peak resistance of the film obeys a power law in the room-temperature sheet resistance with a power of 1.4. This behavior has been seen before in anodized granular NbN films;[15] however, the power varied with the grain size of the films. In the cermets, there was also a power law governing the characteristic resistance R_0 with respect to the room-temperature sheet resistance and the power was also 1.4. Thus, there is a linear relationship between R_0 and the peak resistance.

Figure 6 shows these R_0 resistances for a number of films plotted against the peak resistances R_p. The log-log plot has a slope of 1 over two-and-a-half decades of resistance; the slope of the resistance-versus-$\ln T$ plot *is linearly proportional to the maximum resistance of the film*. This means that high-temperature resistance measurements give information about details of the superconducting transition.

The origins of this logarithmic behavior are unclear. There have been many observations of logarithmic variations of resistance in disordered and reduced dimensionality materials over the years, particularly in systems exhibiting weak localization and/or electron-electron interaction effects. Such behavior has been observed in other cermet systems.[2,11] Nevertheless, a common feature of these systems is that the logarithmic temperature dependence is very weak and occurs over a limited temperature range. In weak-localization theory, the total change in resistance over a decade of temperature is typically on the order of a few percent or less and is certainly no more than about 10%.

In fact, weak-localization theory predicts a value of $\Delta R_\square / R_\square^2$ of approximately 3×10^{-5}, the exact value depending on assumptions made concerning the inelastic-scattering mechanism and the form of interaction contributions.[16] The cermet films studied here show resistance variations 2 orders of magnitude larger than this. In addition, localization theory predicts a crossover from logarithmic to exponential temperature dependence with increasing $R_\square$. This crossover occurs in the range 1–10 k$\Omega/\square$.[17] Therefore, if the logarithmic temperature

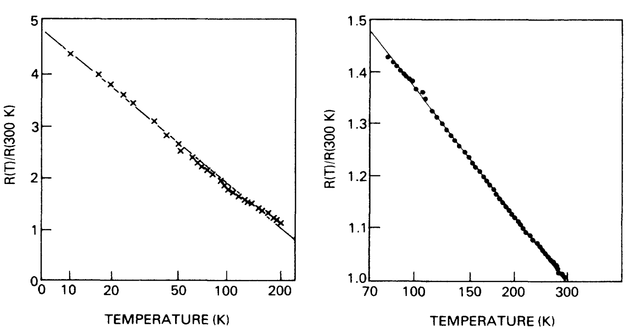

FIG. 5. The resistance normalized to the room-temperature value vs $\ln T$ for two different superconducting samples. The graph on the left is for a sample with $R_\square(300\text{ K}) = 2000\ \Omega/\square$, while that on the right is for $R_\square(300\text{ K}) = 100\ \Omega/\square$. The lines are guides to the eye.

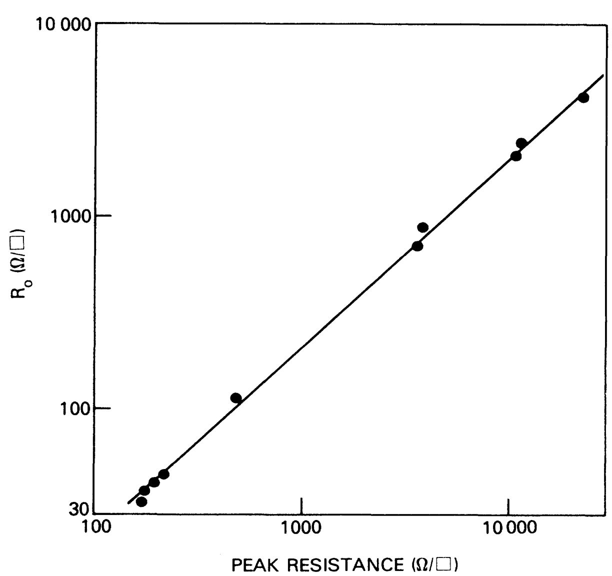

FIG. 6. The logarithm of the coefficient of the $\ln T$ term in Eq. (2) vs the logarithm of the peak resistance for the superconducting samples. The slope on this plot is always unity (corresponding to $R_0 \sim R_p$), but the intercept (corresponding to the ratio R_0/R_p) varies somewhat for samples made at different times.

dependence seen in our films were caused by weak localization, a crossover to exponential behavior should be expected at lower temperatures for the higher-R films. No evidence of this behavior was seen even for films with peak sheet resistance above 20 000 $\Omega/\Box$.

The nature of the transport mechanism remains unknown for these films, but it is clear that there must be Josephson coupling between the grains since the films behave as bulk superconductors. However, tunneling transport between the grains at high temperature does not account for the unusual temperature dependence observed. At this point we can only qualitatively assert the existence of a temperature-dependent tunneling mechanism that results in the logarithmic resistance behavior.

V. SUPERCONDUCTING TRANSITION

The cermet films in the logarithmic group all exhibit superconducting transitions at reduced temperatures. The transitions broaden with increasing sheet resistance and the transition temperature decreases as well. Figure 7 shows three such transitions normalized to the peak resistances of films of room-temperature sheet resistances of 1000, 700, and 300 $\Omega/\Box$. Figure 8 shows the variation of mean-field T_{c0} with sheet resistance. It should be noted that these films reached considerably higher resistances than their room-temperature values before the onset of the superconducting transitions. A 1970-$\Omega/\Box$ room-temperature film reached nearly 22 000 $\Omega/\Box$ at 5 K before dropping to zero resistance at 1.6 K. Thus, for the sample measured (5.8 $\Box$), there was a resistance change of 128 000 Ω over 3.4 K.

The onset of superconductivity in these films can be analyzed in terms of superconducting fluctuations via the Aslamazov-Larkin theory[18] and, in fact, the two-dimensional theory proved to give the best fits to the data. This was in spite of the fact that the films were rather thick (20–50 nm) on the scale of the grain sizes or the superconducting coherence length in NbN. The main departure from the traditional Aslamazov-Larkin fitting procedure that determines a mean-field critical temperature for the film is that the normal-state contribution to the conductivity (σ_n) is usually taken as a constant. Here, such an approximation is quite inappropriate as the normal-state conduction is dominated by the logarithmic interaction discussed above and contributes strong variations in the conductivity over the temperature range of interest. Thus the mean-field T_{c0} of the material is found by fitting the measured conductivity to the form

$$\sigma = \frac{\sigma_0}{\ln(T_0 - T)} + \frac{e^2}{16\hbar}\frac{T_{c0}}{T - T_{c0}}, \tag{3}$$

where σ_0 corresponds to the inverse of R_0 discussed above. Figure 9 shows the results of such a fit for a 1000-($\Omega/\Box$) sample for which T_{c0} is found to be 3.6 K.

The lower part of the superconducting transition in the cermets can be analyzed in terms of the Kosterlitz-Thouless vortex binding-unbinding theory[19] with, in some cases, the addition of charging and/or quantum-fluctuation effects as modeled by Jose[20] and Doniach.[21]

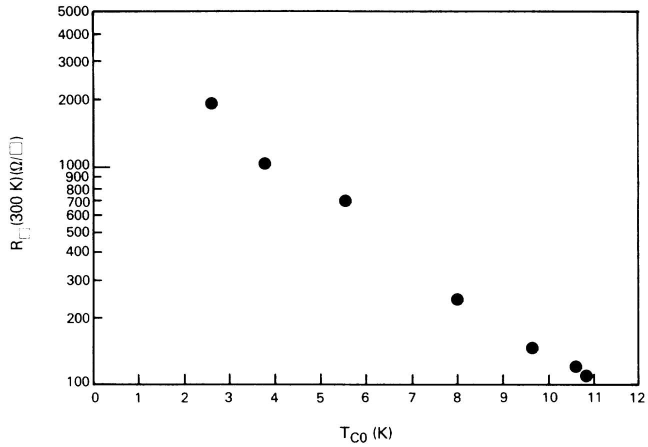

FIG. 8. The room-temperature sheet resistance as a function of the mean-field superconducting transition temperature.

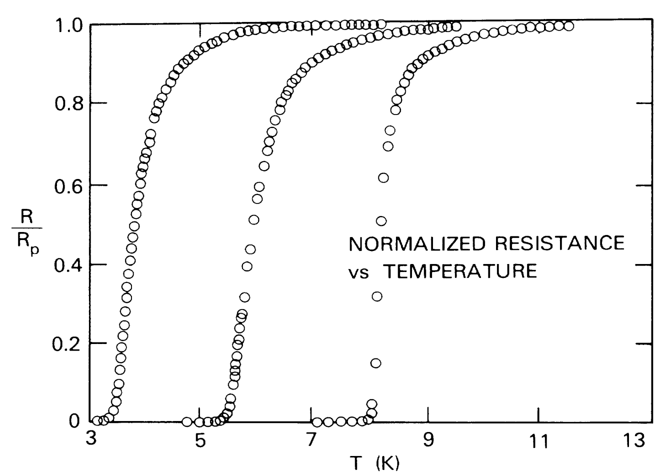

FIG. 7. The resistance, normalized to the peak resistance as a function of temperature, showing the superconducting transition for three samples. As one proceeds from the right the respective room-temperature sheet resistances are 300, 700, and 1000 $\Omega/\Box$.

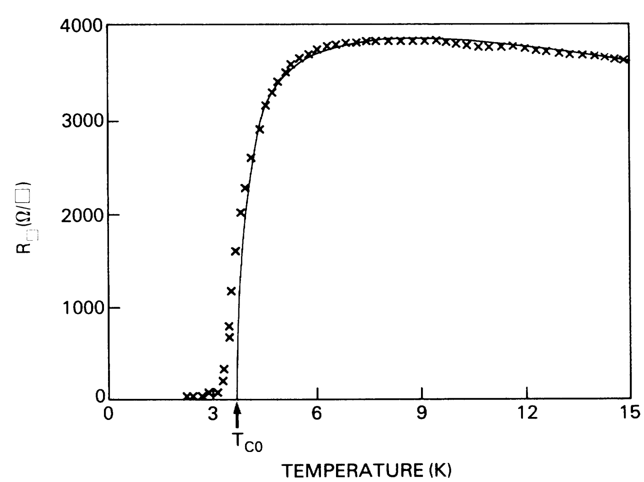

FIG. 9. A fit of the superconducting transition to Eq. (3) for a sample with $R_\Box(300) = 1000\ \Omega/\Box$. The line is the best fit to the data.

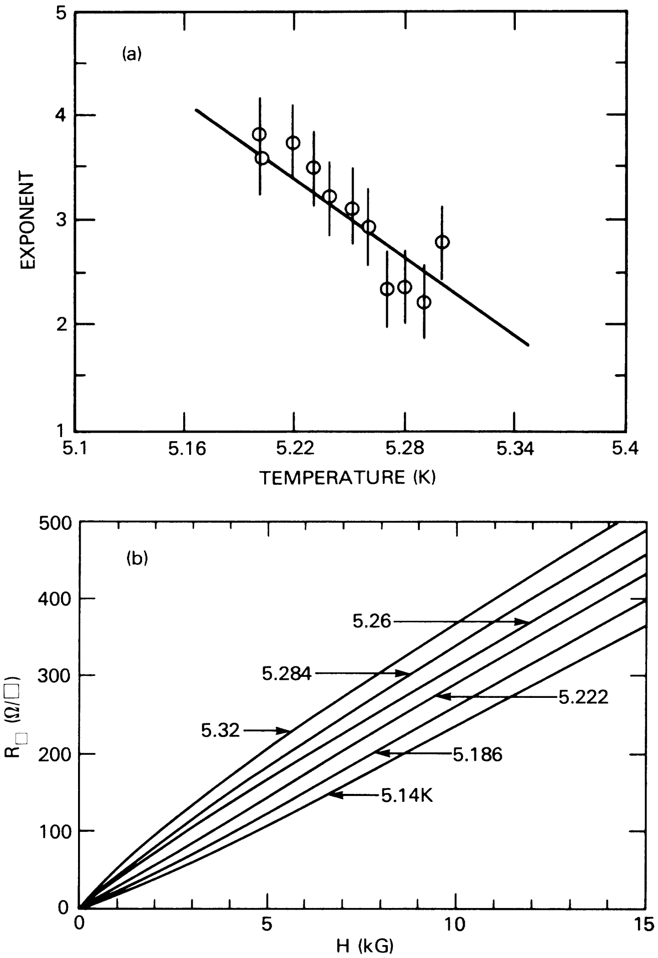

FIG. 10. Two ways of finding T_{2D} are (a) plotting the ν in $V \propto I^{\nu}$ as a function of T and finding where $\nu = 3$, and (b) plotting the resistance as a function of magnetic field for various temperatures and finding where the curve is linear. For this sample both methods give $T_{2D} = 5.24$ K.

Analysis of the contribution of charging effects in these cermets has been reported elsewhere.[22]

The KT transition in these films can be determined quite precisely by two distinct methods. The first utilizes power-law fits to current-voltage characteristics of the film[5,23] for which the relationship $V \sim I^3$ holds at T_{2D}. Figure 10(a) shows the power for the current-voltage dependence (taken from the slope of log-log plots of I-V characteristics) plotted as a function of temperature for a typical sample. The temperature for which the power is three is taken to be T_{2D}, in this case 5.24 K.

The second technique involves the use of flux-flow–resistance data.[24] Figure 10(b) shows a family of magnetoresistance isotherms for the same sample as in Fig. 10(a). As the temperature increases from 5.14 up to 5.32 K, the curves progress from positive curvature through linear behavior to negative curvature. Below T_{2D} field-induced free vortices dominate the magnetoconductance, which results in the superlinear response to the applied field. Above T_{2D} thermally induced vortices dominate and the additional vortices induced by the field result in only a sublinear response. However, at T_{2D} the vortex-antivortex correlation length diverges and pure flux-flow resistance is observed. Thus the linear isotherm occurs at the transition temperature. Agreement between the two measurements is quite good for these samples.

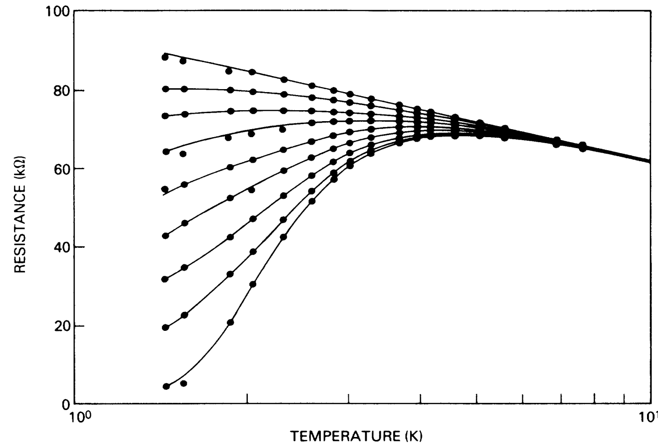

FIG. 11. The resistance as a function of temperature (plotted as $\ln T$) for a variety of magnetic fields with values of 0, 10, 20, 30, 40, 50, 60, 70, and 80 kG. Note that when the superconductivity has been quenched, the $\log_{10} T$ dependence seen at higher temperatures has been recovered. This sample had $R_{\square}(300\text{ K}) = 2000\ \Omega/\square$.

VI. OTHER RESULTS AND DISCUSSION

The magnetoresistance measurements performed for the T_{2D} analysis above led to several other interesting observations. As mentioned earlier, if a magnetic field sufficiently high to suppress superconductivity is applied, the logarithmic temperature dependence of the resistivity can be observed down to low temperatures. Figure 11 shows the gradual destruction of superconductivity with applied field on a 2000-$\Omega/\square$ sample. At the highest field, one sees the continuation of the logarthmic behavior.

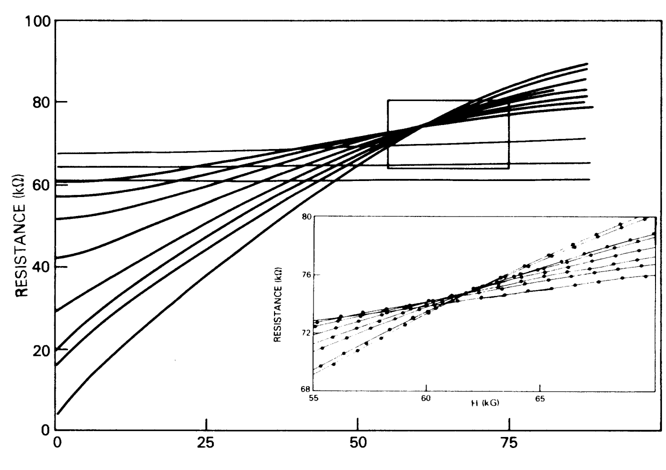

FIG. 12. The resistance as a function of magnetic field for various temperatures. Note that at $H \approx 60$ kG the resistance appears independent of temperature. The inset is an expansion of the data in the box. This sample has $R_{\square}(300\text{ K}) = 2000\ \Omega/\square$.

Thus we observe this remarkable temperature dependence over two decades of temperature.

It is interesting to note in Fig. 11 that for a field of 6T the resistance-versus-temperature curve is flat below 15 K. This can be seen very clearly in Fig. 12, in which all the field isotherms meet at one point. It appears that at this particular value of field (actually 6.2 T), the superconductivity and the logarthmic transport mechanism exactly cancel out, and there is no temperature dependence of the resistivity. More careful examination of the data shows the resistance to be constant to within better than 1% below the peak in resistivity at this field value. Such a crossing of magnetoresistance isotherms has been seen before,[25] but it is unclear in this case whether it is merely a coincidence or is actually instructive about the conduction mechanisms in these cermet films.

We have fabricated and performed transport measurements in a novel cermet system composed of co-sputtered NbN and BN. Insulating samples within this system provide for the study of modified hopping transport. Superconducting samples provide an excellent model for the 2D Kosterlitz-Thouless phase transition and, in addition, also exhibit a unique wide-ranging logarithmic temperature dependence of resistivity in the normal state. While the films studied here are amenable to analysis as two-dimensional films, the fabrication techniques can allow for much thicker films to be produced, so that the effects of dimensionality can be studied in detail. As in other granular systems, these cermets make good bolometric detectors,[26] and have also recently been shown to be very sensitive radiation detectors in the superconducting state by a nonequilibrium mechanism.[27] Work is continuing in a number of areas on these films.

ACKNOWLEDGMENTS

The authors wish to thank K. E. Kihlstrom, J. H. Claassen, and D. U. Gubser, as well as A. F. Hebard and A. M. Goldman, for useful discussions and assistance in the course of this work. We also wish to thank Alan M. Kadin for many helpful comments and suggestions on this paper.

*Present address: TRW Space & Technology Group, One Space Park, Redondo Beach, CA 90278.

[1]T. J. Coutts, Thin Solid Films **38**, 313 (1976).
[2]T. Chui, G. Deutscher, P. Lindenfeld, and W. L. McLean, Phys. Rev. B **23**, 6172 (1981).
[3]S. A. Wolf, D. U. Gubser, W. W. Fuller, J. C. Garland, and R. S. Newrock, Phys. Rev. Lett. **47**, 1071 (1981).
[4]A. F. Hebard and A. T. Fiory, Phys. Rev. Lett. **44**, 291 (1981).
[5]K. Epstein, A. M. Goldman, and A. M. Kadin, Phys. Rev. Lett. **47**, 534 (1981).
[6]A. F. Hebard and M. A. Paalanen, Phys. Rev. B **30**, 4063 (1984).
[7]S. A. Wolf and W. H. Lowrey, Phys. Rev. Lett. **39**, 1038 (1977).
[8]O. P. Agnihotri and B. K. Gupta, *Solar Selective Surfaces* (Wiley, New York, 1981), p. 161.
[9]B. Abeles, P. Sheng, M. D. Coutts, and Y. Arie, Adv. Phys. **24**, 407 (1975).
[10]R. W. Cohen, C. D. Cody, M. D. Coutts and B. Abeles, Phys. Rev. B **8**, 3689 (1973).
[11]J. Affinito, N. Fortier, and R. R. Parsons, J. Vac. Sci. Technol. A **2**, 316 (1984).
[12]J. I. Gittleman, Y. Goldstein, and S. Bozowski, Phys. Rev. B **5**, 3609 (1972).
[13]A. L. Efros and B. Shklowskii, J. Phys. C **8**, L49 (1975).
[14]O. Entin-Wohlman, Y. Gefen, and Y. Shapira, J. Phys. C **16**, 1161 (1981).
[15]D. U. Gubser and S. A. Wolf (unpublished).
[16]S. Kobayashi, in *Localization, Interaction, and Transport Phenomena,* edited by B. Kramer, G. Bergmann, and Y. Bruynseraede (Springer-Verlag, Berlin, 1985), p. 18.
[17]G. J. Dolan and D. D. Osheroff, Phys. Rev. Lett. **43**, 721 (1979).
[18]L. G. Aslamazov and A. I. Larkin, Fiz. Tverd, Tela (Leningrad) **10**, 1104 (1968). [Sov. Phys.—Solid State, **10**, 875 (1968)].
[19]J. M. Kosterlitz and D. J. Thouless, J. Phys. C **6**, 1181 (1973).
[20]J. V. Jose, Phys. Rev. B **29**, 2836 (1984).
[21]S. Doniach, in *Percolation Localization, and Superconductivity,* edited by A. Goldman and S. Wolf (Plenum, New York, 1984), p. 401; also in Phys. Rev. B **24**, 5063 (1981).
[22]D. U. Gubser, S. A. Wolf, W. W. Fuller, D. Van Vechten, and R. W. Simon, Physica (Utrecht) 135B, 131 (1985).
[23]B. I. Halperin and D. R. Nelson, J. Low Temp. Phys. **36**, 599 (1979).
[24]A. T. Fiory, A. F. Hebard, and W. I. Glaberson, Phys. Rev. B **23**, 5075 (1983).
[25]B. J. Dalrymple (unpublished); A. F. Hebard (private communication).
[26]K. Weiser, U. Strom, S. A. Wolf, and D. U. Gubser, J. Appl. Phys. **52**, 4888 (1981).
[27]M. Leung, U. Strom, R. W. Simon, and S. A. Wolf, in Proceedings of the 1986 Applied Superconductivity Conference, Baltimore, 1986 [IEEE Trans. Magn. MAG-**23**, (1987)].

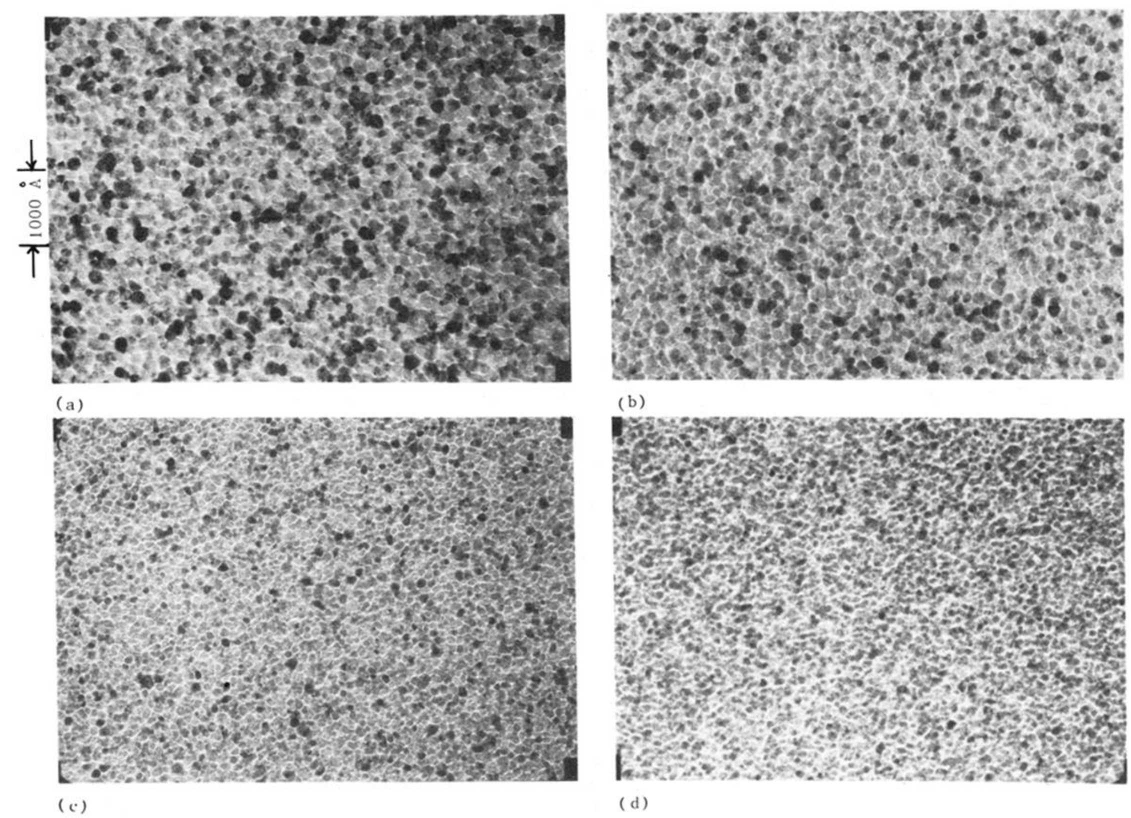

FIG 2. Micrographs of films at four different substrate locations. The substrate positions as referred to Fig. 1 are (a) 2, (b) 3, (c) 4, and (d) 5.